Li, Yun; Chen , Yongming ; Tang, Chaobo; Yang, Shenghai ; Klemettinen, Lassi; Rämä, Minna; Wan, Xingbang; Jokilaakso, Ari

A New Pyrometallurgical Recycling Technique for Lead Battery Paste without SO2 Generation

Published in:
Extraction 2018

DOI:
10.1007/978-3-319-95022-8_90

Published: 01/01/2018

Document Version
Peer-reviewed accepted author manuscript, also known as Final accepted manuscript or Post-print

Published under the following license:
Unspecified

Please cite the original version:
Li, Y., Chen , Y., Tang, C., Yang, S., Klemettinen, L., Rämä, M., Wan, X., & Jokilaakso, A. (2018). A New Pyrometallurgical Recycling Technique for Lead Battery Paste without SO2 Generation: A Thermodynamic and Experimental Investigation. In *Extraction 2018: Proceedings of the First Global Conference on Extractive Metallurgy* (pp. 1109-1120). (The Minerals, Metals & Materials Series). Springer. https://doi.org/10.1007/978-3-319-95022-8_90

A new pyrometallurgical recycling technique for lead battery paste without SO_2 generation—a thermodynamic and experimental investigation

Yun Li [1,2], Yongming Chen[2], Chaobo Tang[2], Shenghai Yang[2], Lassi Klemettinen[1], Minna Rämä[1], Xingbang Wan[1], Ari Jokilaakso[1,*]

1. *Aalto University, School of Chemical Engineering, Department of Chemical and Metallurgical Engineering, Espoo, 02150, Finland*
2. *School of Metallurgy and Environment, Central South University, Changsha, Hunan, 410083, P.R China*

*Corresponding author: Ari Jokilaakso, e-mail: ari.jokilaakso@aalto.fi; tel: +358 503138885. Yun Li, e-mail: yun.li@aalto.fi, tel: +358 469201618; Yongming Chen, e-mail: csuchenyongming@163.com, tel: +86 18684685548; Chaobo Tang, e-mail: chaobotang@163.com; tel: +86 13875801550; Shenghai Yang, e-mail: yangshcsu@163.com; tel: +86 13975894838; Lassi Klemettinen, e-mail: lassi.klemettinen@aalto.fi; tel: +358 44 2149569; Minna Rämä, e-mail: minna.rama@aalto.fi; tel: +358 505264301; Xingbang Wan, e-mail: xingbang.wan@aalto.fi; tel: +358503240975.

Abstract

An innovative lead recycling process from scrap lead-acid battery paste is presented. The novelty in the process is avoiding SO_2 generation and emission by using reductive sulfur-fixing technique. Iron-bearing secondary wastes produced from metallurgical industry were utilized as sulfur-fixing agent to capture sulfur in the form of FeS (s) instead of generation of SO_2 (g). Molten Na_2CO_3 salt was added to the smelting system to speed the reactions and improve valuable metals' recovery and sulfur-fixation efficiency. Furthermore, this process can simultaneously co-treat various lead and iron-bearing wastes. At the same time, some precious metals, such as Au and Ag, contained in iron-bearing wastes can be recovered. The feasibility and reliability of this process was investigated thermodynamically and experimentally with the help of HSC 9.0 database and XRD and SEM-EDS analysis. A possible reaction mechanism and path in $PbSO_4$-Fe_2O_3-Na_2CO_3-C smelting system was also clarified.

Key words: Reductive sulfur-fixing smelting; Co-treatment; Iron-bearing wastes; Sulfur-fixing agent; SO_2 (g) emission free; Precious metals' recovery; Reaction mechanism.

1. Introduction

Lead (Pb) is a very important metal for our daily life. It is widely used in e.g. lead-acid batteries (LAB), cables, as a soldering flux and as PVC stabilizer [1, 2]. However, during recent years, with the rapid development of auto, energy transportation and telecommunication industries[3], more than 85% of global pure lead production is applied to LAB manufacturing [4]. As a result, more than 6 million tons of LABs were scrapped annually worldwide [1]. Scrap LABs have recently become significant secondary lead sources globally [5, 6]. Secondary lead produced by various recycling processes has dominated world's lead production market [7].

Currently, scrap LAB recycling technology primarily includes pyrometallurgy and hydrometallurgy. Pyrometallurgy [8] is globally the predominant methodology for spent LAB recycling. Meanwhile, reverberatory furnaces, blast furnaces, electric furnaces or rotary furnaces are usually selected to smelt lead paste [9]. However, in the hydrometallurgical process, typically, a pre-desulfuration procedure is necessary. In this procedure, Na_2CO_3, NaOH, K_2CO_3 solutions or citric acid and citrate salt are usually adopted as desulfuration reagents [10]. In addition, some emerging technologies, including solid phase electrolysis [11], biological technique [12], and vacuum methods [13] etc., are being developed and applied steadily. However, some problems still exist and need to be solved, such as lead-containing dust and SO_2 emission in pyrometallurgy, as well as tedious procedures and large amount of unmanageable waste water generation in hydrometallurgy. A cleaner and more efficient lead recycling technology is urgently needed for handling the growing amount of lead-bearing secondary raw materials [5, 14, 15].

In this study, an innovative lead recycling technology, referred to as reductive sulfur-fixing smelting, was proposed and investigated through thermodynamic calculations and lab-scale experiments. The lab-

scale experiments were conducted to investigate the reaction mechanism in $PbSO_4$-Fe_2O_3-Na_2CO_3-C system. In addition, XRD and SEM-EDS analyses were employed to characterize phase transformations and microstructural changes.

2. Experimental

2.1 Materials

The lead paste was supplied by Yuguang Gold & Lead Co., Henan, China. The sulfur-fixing agent, jarosite residue, was obtained from Xingan Copper & Lead Co., Inner Mongolia, China. The reductive agent, metallurgical coke, was supplied by Xiangtan Iron & Steel Co., Ltd of Hunan Valin, China. The chemical compositions of these materials were analyzed by Inductively Coupled Plasma-Atomic Emission Spectrometry (Perkin Elmer, Optima 3000 ICP-AES). The results are shown in Table 1. The materials employed in reaction mechanism experiments, including $PbSO_4$, Fe_2O_3, Na_2CO_3 and carbon, were of analytical grade (≥ 99.99%) and purchased from Aladdin Industrial Corporation, China. Argon was used as a protective gas with a purity of 99.99%.

Table 1 Chemical composition of the corresponding materials.

Materials	ICP-AES analysis results /wt.%													
Lead paste	Pb	S	Si	Ba	Ca	Fe	Na	Zn	Mg	Al	Nd	Cu	K	Ag
	68.81	3.33	3.52	0.16	0.55	0.05	0.97	--	0.16	0.16	0.13	0.02	0.06	--
Jarosite residue	Pb	S	Si	Ba	Ca	Fe	Na	Zn	Mg	Al	Nd	Cu	K	Ag
	0.32	13.00	2.12	--	0.76	24.30	--	2.30	--	0.91	--	0.13	0.05	0.005
Coke	Industrial analysis /wt.%			Chemical composition of the ash/%										
	Fixed Carbon		Volatile	Ash	Fe_{total}	SiO_2	CaO	Al_2O_3	MgO					
	81.27		3.30	15.43	25.23	41.23	6.60	25.24	0.53					

2.2 Methods

Fig. 1 shows a schematic diagram of the experimental apparatus. In the smelting experiments of lead paste, 200 g of lead paste was mixed evenly with the given amount (presented in chapter 4.1.) of coke, jarosite residue, Na_2CO_3 and other fluxes in every test, and the mixture was placed into a weighed 150 ml alumina crucible. The crucible was positioned in the constant temperature zone of the furnace after removing the air by Ar gas when the temperature was raised to the desired value and held for a preset time. After the required smelting time, the crucible was taken out from the furnace and quenched rapidly in liquid nitrogen and weighed. Next, the crucible was broken to carefully separate and weigh crude lead, ferrous matte and slag. Each of the samples was crushed and well-prepared for analysis. The chemical compositions of each sample were analyzed by ICP-AES. The lead recovery and sulfur-fixing rates were calculated based on mass balance.

In the reaction mechanism experiments, the materials were finely mixed according to the stoichiometric number of their possible reactions. The mixtures were pressed under 15MPa pressure to obtain cylindrical samples having a diameter of 10 mm. The samples were put into a 10 ml alumina crucible, and placed into the constant temperature zone of the furnace when temperature was raised to the desired value after removing the air and held for preset time. The temperature was measured with a Pt–Rh thermocouple and controlled using a Japan SHIMADEN SR25 Intelligent Temperature Controller (accuracy ± 1°C). The protective Ar gas inlet flow rate was fixed at 1.0 L/min. Each product was also quenched rapidly in liquid nitrogen. The phase compositions and microstructure of every sample were characterized by XRD and SEM-EDS, respectively.

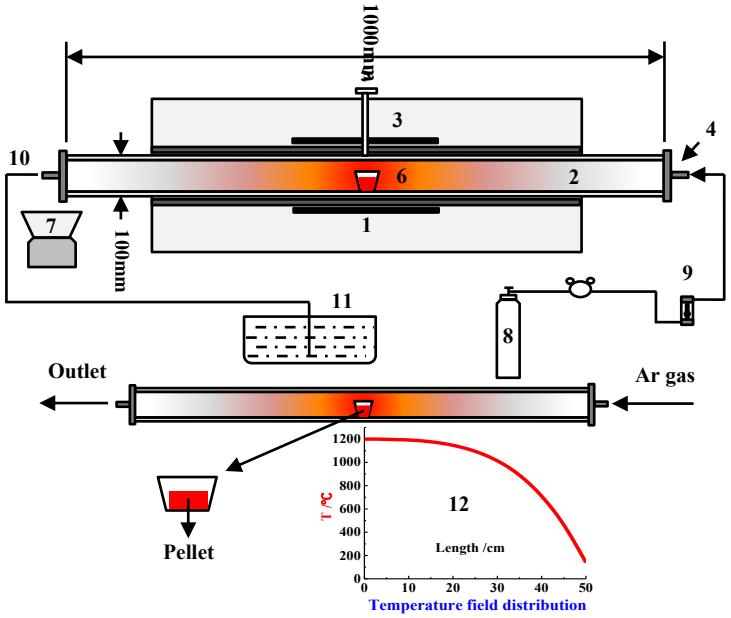

1. Horizontal electric resistance tube furnace; **2.** Corundum tube; **3.** Heating units; **4.** Sealing flange; **5.** Pt-Rh thermocouple; **6.** Corundum crucible; **7.** Liquid nitrogen cooling device; **8.** N_2 gas cylinder; **9.** Flowmeter; **10.** Tail gas; **11.** Alkali liquor vessel; **12.** Temperature field distribution in corundum tube.

Fig. 1 Schematic diagram of the experimental apparatus.

3. Thermodynamics

A metallurgical process is a complex multi-phenomena system. It is difficult to observe directly the various physical and chemical reactions during high temperature smelting. However, metallurgical thermodynamics can calculate and investigate the feasibility, direction and limitations of reactions and the form of the products. For example, the predominance-area diagram can intuitively tell us the smelting conditions for producing the desired metallurgical products and how to provide and optimize these conditions. Therefore, metallurgical investigators can avoid tedious thermodynamic calculations by using HSC Chemistry Software [16]. Table 2 lists the possible reactions that may take place during the smelting process.

Table 2 Possible reactions in the lead paste reductive sulfur-fixing smelting process.

Reactions	$\Delta G_T^\theta - T$ **(kJ/mol)**[16]	**Eq.**
$PbSO_4 + 4\ C = PbS + 4\ CO\ (g)$	$\Delta G_T^\theta = -0.681T + 166.39$	(1)
$PbSO_4 + C = PbO + CO(g) + SO_2\ (g)$	$\Delta G_T^\theta = -0.34T + 186.33$	(2)
$PbS + 2\ PbO = 3\ Pb + SO_2\ (g)$	$\Delta G_T^\theta = -0.191T + 169.25$	(3)
$PbO + C = Pb + CO\ (g)$	$\Delta G_T^\theta = -0.177T + 49.77$	(4)
$2\ PbSO_4 + Fe_2O_3 + 11\ C = 2Pb + 2\ FeS + 11\ CO\ (g)$	$\Delta G_T^\theta = -1.951T + 667.96$	(5)
$3\ PbSO_4 + Fe_3O_4 + 16\ C = 3\ Pb + 3\ FeS + 16\ CO\ (g)$	$\Delta G_T^\theta = -2.808T + 964.2$	(6)
$2\ PbS + Fe_2O_3 + 3\ C = 2\ Pb + 2\ FeS + 3\ CO\ (g)$	$\Delta G_T^\theta = -0.589T + 335.2$	(7)
$3\ PbS + Fe_3O_4 + 4\ C = 3\ Pb + 3\ FeS + 4\ CO\ (g)$	$\Delta G_T^\theta = -0.765T + 465.04$	(8)
$PbSO_4 + Na_2CO_3 + 6\ C = Pb + Na_2S + 7\ CO\ (g)$	$\Delta G_T^\theta = -1.164T + 538.2$	(9)
$PbSO_4 + Na_2CO_3 + 2\ C = Pb + Na_2SO_4 + 3\ CO\ (g)$	$\Delta G_T^\theta = -0.501T + 178.61$	(10)
$PbS + Na_2CO_3 + 2\ C = Pb + Na_2S + 3\ CO\ (g)$	$\Delta G_T^\theta = -0.483T + 371.8$	(11)

Fig. 2 illustrates diagrams of the relationships between ΔG_T^{θ}, CO% and T during reductive sulfur-fixing smelting process. Fig. 2(a) suggests that the reactions (5)-(11) could take place spontaneously at the smelting temperature range, and increasing the temperature would promote these reactions. The reductive equilibrium diagrams of $PbSO_4$ and Fe_2O_3 in Fig. 2 (b) and (c) further illustrate that four stable primary areas, $PbSO_4$, PbS, PbO and Pb, exist at different reductive atmospheres at the test temperature. At relatively low temperatures, $PbSO_4$ could be easily reduced into PbS under a weak reductive atmosphere. However, with increasing temperature, $PbSO_4$ prefers to be reduced to PbO. Furthermore, if the reducing atmosphere would be stronger, PbO could continually be reduced to metallic Pb. Nevertheless, in practice, continuous reduction of PbS into metallic Pb was difficult [17]. But according to reaction (3), PbS could also react with PbO to generate metallic Pb. In addition, Fig. 2 (b) and (c) also reveal that, at the range of smelting temperature and reductive atmosphere, Fe_2O_3 would be reduced into and mainly stable in the form of Fe_3O_4.

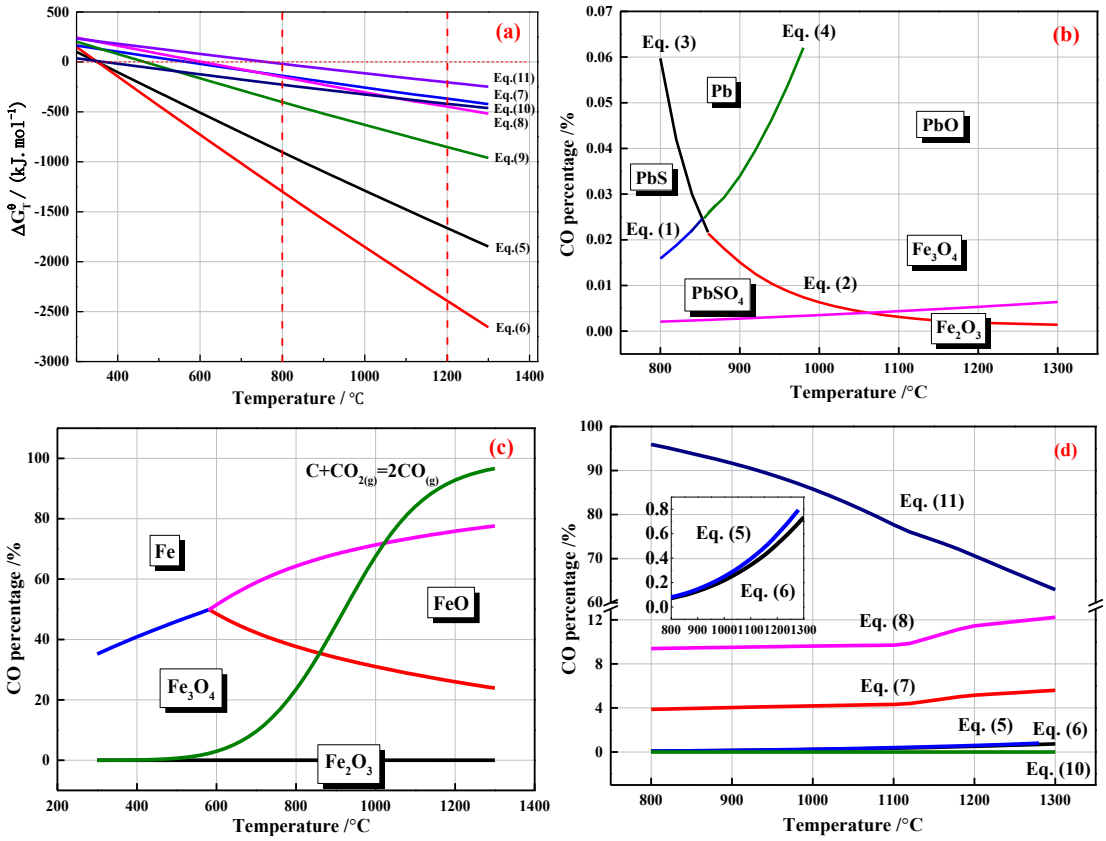

Fig. 2 Thermodynamic diagrams of the investigated smelting system.

Fig. 2 (d) shows the reductive equilibrium diagram of reactions between $PbSO_4$, PbS and Fe_xO_y, Na_2CO_3. It suggests that, at the presence of molten Na_2CO_3 salt and sulfur-fixing agent Fe_2O_3, $PbSO_4$ could easily react with Na_2CO_3 in the smelting temperature range. Moreover, Fe_3O_4 would also react with $PbSO_4$ and PbS to generate FeS, and, as a result, sulfur would be transferred from $PbSO_4$ to Na_2SO_4 and FeS. The results also suggest that $PbSO_4$ is more likely to react with Na_2CO_3 and Fe_xO_y than PbS at the smelting conditions.

4. Results and discussion

4.1 Effect of coke and Na_2CO_3 addition on lead recovery and sulfur-fixing rate

Fig. 3(a) depicts the effect of coke and Na_2CO_3 dosage on lead recovery and sulfur-fixing rate in the lead paste reductive sulfur-fixing smelting process. The proportion of raw materials was $W_{\text{lead paste}}$: $W_{\text{jarosite residue}}$: W_{Na2CO3} =200:40:36. FeO/SiO_2 and CaO/SiO_2 ratio were fixed at 1.0 and 0.5, respectively. Each sample was smelted at 1200 °C for 2 h. The results showed that the lead recovery and sulfur-fixing rates increased from 4% to 8% of coke addition and peaked at 8% where 91.0% of lead was recovered

and enriched in crude lead, and 92.6% of sulfur was fixed in ferrous matte and slag. However, as the coke addition continued increasing, the lead recovery and sulfur-fixing rates tended to decrease simultaneously. At the same time, the amount of lead lost in the slag phase decreased steadily. This indicates that lead tended to volatilize when reductivity of the atmosphere became stronger. In addition, the sulfur-fixing products, Na_2SO_4 and Na_2SO_3, would also be reduced-decomposed under a strongly reductive atmosphere. Therefore, the sulfur-fixing rate exhibited a gradually decreasing trend with the increasing coke addition.

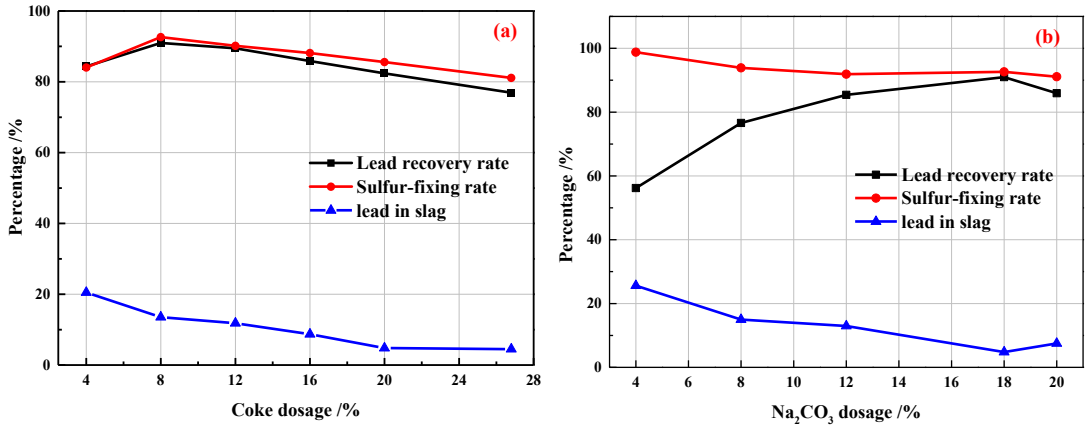

Fig. 3 Effects of coke (a) and Na_2CO_3 (b) dosage on lead recovery and sulfur-fixing rates.

The influence of Na_2CO_3 dosage on the lead recovery and sulfur-fixing rates are presented in Fig. 3(b). In these experiments, the proportion of raw materials was $W_{lead\ paste}$: $W_{jarosite\ residue}$: W_{Coke} =200:40:16. FeO/SiO_2 and CaO/SiO_2 ratio were fixed at 1.0 and 0.5, respectively. Each sample was carried out at 1200 °C for 2 h. It was observed from the results that the lead recovery increased steadily from 56.2% to 91.0%, and the amount of lead lost in the slag decreased gradually, and only 4.8% of lead was lost in the slag with 18% Na_2CO_3 addition. The presence of Na_2CO_3 decreases the viscosity of the melt and increases its fluidity [18]. Therefore, more metallic lead was generated during smelting. However, the lead recovery presents a weak decrease after 18% of Na_2CO_3 addition because excess addition of Na_2CO_3 would increase the output of matte and slag and increase the total dissolved losses of lead in them. Sulfur-fixing rate showed a slight decline with the increasing Na_2CO_3 dosage Nevertheless, 91.1%-98.8% of sulfur was fixed in the matte and slag with varying Na_2CO_3 addition. In conclusion, the results imply that a suitable Na_2CO_3 dosage was found, and that too high Na_2CO_3 addition changes the properties of the melt in a direction that is unbeneficial to lead recovery and sulfur fixation rates [18].

4.2 Reaction mechanism in $PbSO_4$+Fe_2O_3+Na_2CO_3+C system

The results of reaction mechanism investigations in $PbSO_4$-Fe_2O_3-Na_2CO_3-C system are presented in Fig. 4. When the mixture had reacted at 500 °C for 30 min, a part of $PbSO_4$ changed to $Pb_2O(SO_4)$ phase. When the temperature was increased to 650 °C, the generation of lead oxide phases (PbO, Pb_2O and Pb_5O_8) increased. Furthermore, metallic Pb was detected in the product, and some $PbSO_4$ was also reduced to PbS. In addition, sulfur-fixing products, Na_2SO_4 and $NaFeS_2$, were also detected in the product. At 750 °C, more PbS phase was generated and some of the lead oxide reacted with Fe_2O_3 to form a new phase $PbFe_4O_7$. However, $Pb_2O(SO_4)$, $PbSO_4$, Fe_2O_3, PbO and Pb were the main stable phases in the product at 750 °C. When the temperature was increased to 850 °C, $PbSO_4$, $Pb_2O(SO_4)$, Fe_2O_3, $NaFeS_2$ and Pb_5O_8 phases disappeared, and FeS, Fe_3O_4, $PbFe_{12}O_{19}$, $Pb_2Fe_2O_5$, Pb_2O_3 and $Na_5(CO_3)(SO_4)_2$ phases formed. The main phases in the product were PbS, Pb and Na_2SO_4. At 950 °C, the amount of PbS phase decreased significantly and more Na_2SO_4 was generated. Some of the iron-lead oxide phases disappeared. When the temperature rose to 1000°C, the final product was mainly stable in the form of Na_2SO_4, PbS, Pb, Fe_3O_4 and $Na_6Fe_2(SO_4)(CO_3)_4$.

The XRD patterns of products reacted at 850 °C for different times are presented in Fig. 4 (b). After 5 min at 850 °C, the main phases in the product were $Pb_2O(SO_4)$, PbS, PbO, Pb, Na_2SO_4 and Fe_2O_3.

Na_2CO_3 had reacted with $PbSO_4$ and sulfur was fixed in Na_2SO_4. When the reaction time was extended to 10 min, more PbS and Na_2SO_4 were generated, some of the Fe_2O_3 was reduced into Fe_3O_4, and FeS phase appeared. Furthermore, after 15 min, the generation of metallic Pb and Fe_3O_4 increased, and the $Pb_2O(SO_4)$ and Fe_2O_3 phases disappeared. When the reaction time was prolonged to 20 min, $PbFe_{12}O_{17}$, $Na_5(CO_3)(SO_4)_2$, and Pb_2O_3 phases were detected, and they were also stable in the product of the 30 min experiment.

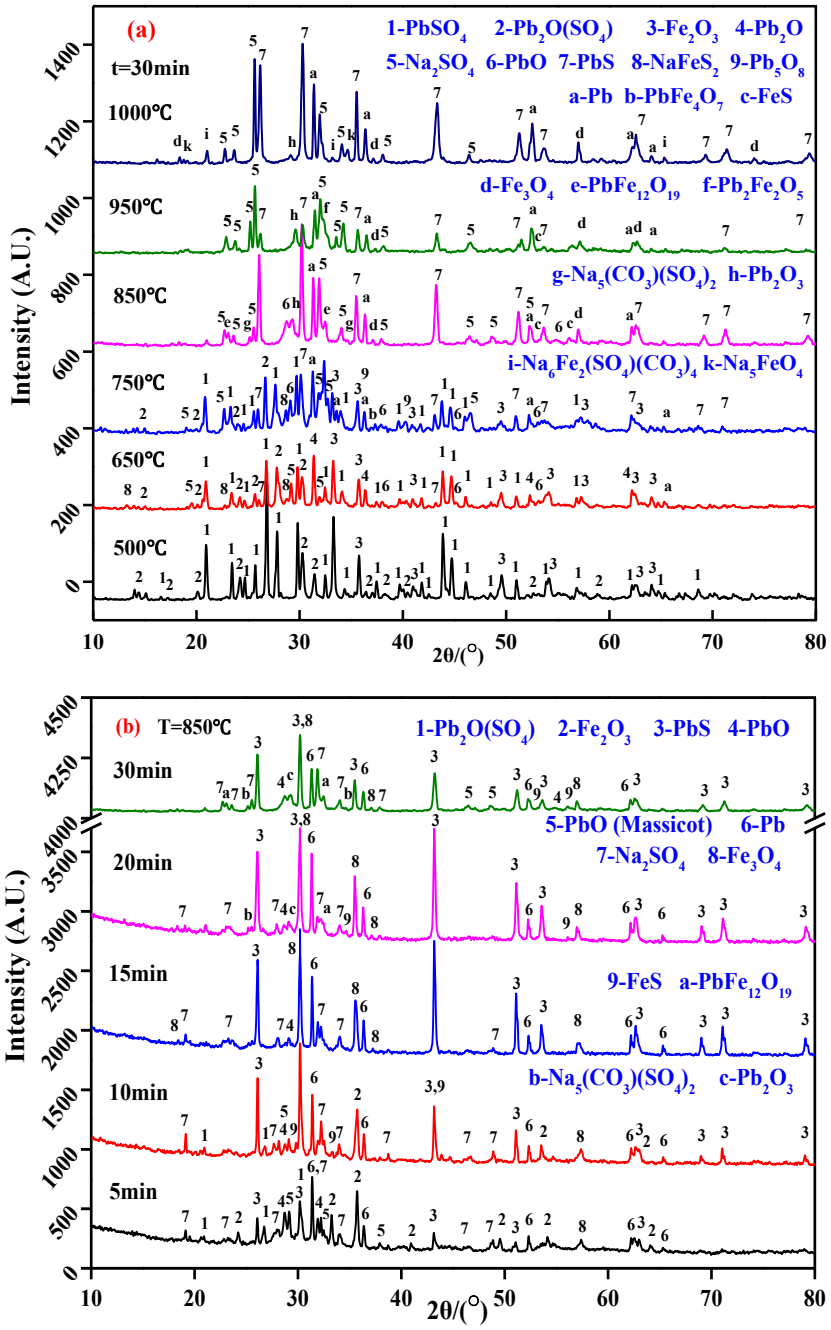

Fig. 4 XRD patterns of products in $PbSO_4$-Fe_2O_3-Na_2CO_3-C (molar ratio 2:1:2:12) reaction system at (a) different temperatures and (b) with different reaction times.

4.3 SEM-EDS analysis of a product in $PbSO_4$+Fe_2O_3+Na_2CO_3+C system

The sample produced from $PbSO_4$-Fe_2O_3-Na_2CO_3-C reaction system at 1000 °C after 30 min was further characterized by SEM-EDS technique. The results are presented in Fig. 5.

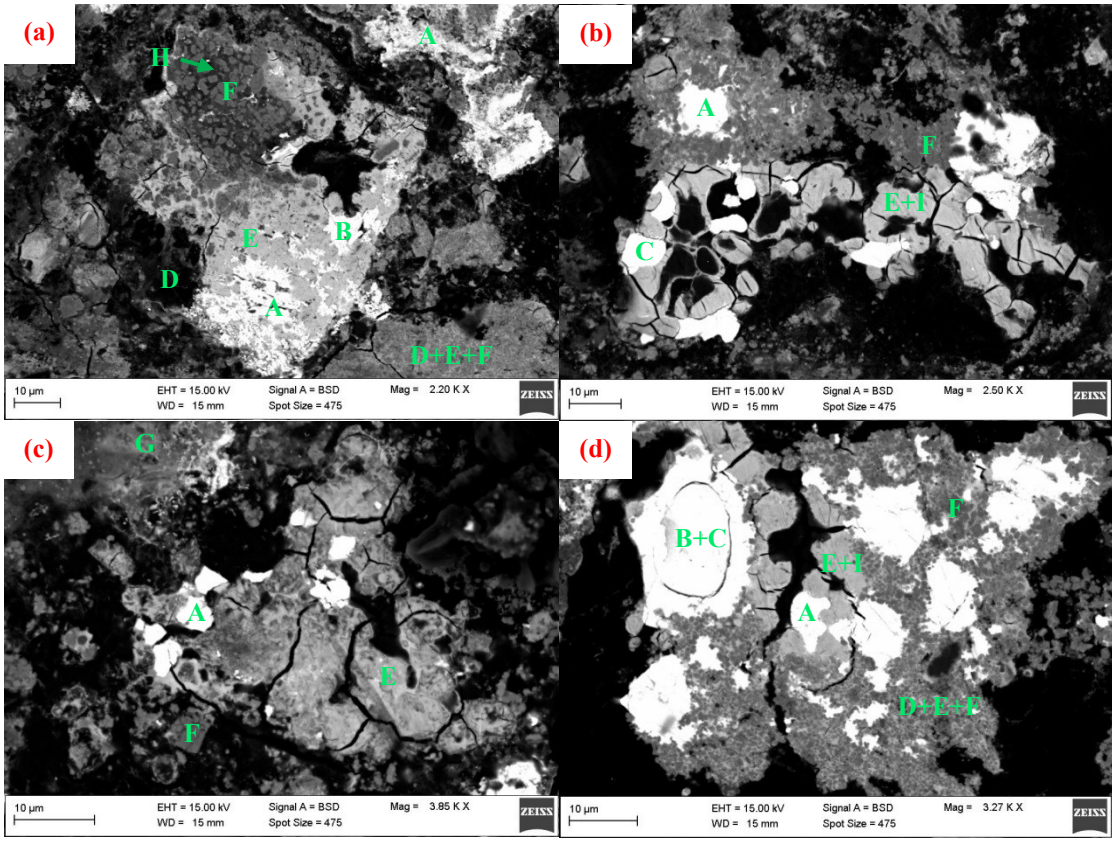

A: Lead sulfide; **B:** Lead oxide; **C:** Metallic lead; **D:** Sodium sulfate; **E:** Lead iron oxide; **F:** Magnetite; **G:** Sodium iron sulfate carbonate; **H:** Sodium iron oxide **I:** Sodium iron sulfide

Fig. 5 SEM-EDS analysis results of products in $PbSO_4$-Fe_2O_3-Na_2CO_3-C (molar ratio 2:1:2:12) reaction system at 1000 °C with 30 min reaction time.

It was observed that the product after 30 min reaction time at 1000 °C still contained some unreacted PbS and Fe_3O_4 due to too short reaction time. The PbS particles were generally surrounded by Fe_3O_4 diffusion barrier. Meanwhile, Na_2SO_4, PbO, $PbFe_xO_y$ and $NaFeS_2$ were detected around the PbS and Fe_3O_4 particles. This indicated that reaction (12) took place between $PbSO_4$ and Na_2CO_3. Na_2SO_4 and PbO phases were gradually generated. Moreover, the reduction product PbS continued to react with iron oxides, mainly Fe_3O_4, to produce PbO and FeS (reaction (13) and (14)). Furthermore, lead oxide was continually reduced by carbon into metallic lead. However, lead oxide also tended to combine with iron oxide, which hindered the further reduction of lead oxide.

$$PbSO_4 + Na_2CO_3 = Na_2SO_4 + PbO + CO_2\,(g) \qquad \Delta G_T^\theta = -0.149T + 6.23\ (\text{kJ/mol}) \qquad (12)$$

$$6\,PbS + 2\,Fe_3O_4 + C = 6\,PbO + 6\,FeS + CO_2\,(g) \qquad \Delta G_T^\theta = -0.292T + 508.86\ (\text{kJ/mol}) \qquad (13)$$

$$4\,PbS + 2\,Fe_2O_3 + C = 4\,PbO + 4\,FeS + CO_2\,(g) \qquad \Delta G_T^\theta = -0.294T + 348.69\ (\text{kJ/mol}) \qquad (14)$$

5. Conclusion

Recycling lead from spent lead-acid battery paste through the reductive sulfur-fixing smelting technique using jarosite residue as sulfur-fixing agent is found thermodynamically and experimentally of be feasible. During the smelting process, $PbSO_4$ tended to react first with Na_2CO_3 to generate PbO and Na_2SO_4, but also to be reduced into PbS. Moreover, Fe_3O_4, a reduction product from Fe_2O_3, could also react with $PbSO_4$ and PbS to generate FeS. Sulfur would be fixed in solid state in the form of FeS and Na_2SO_4, which avoided the SO_2 (g) generation and emissions. The results of the lab-scale lead paste smelting experiments demonstrated that 91.0% of lead could be directly recovered in the crude lead phase,

and up to 98.8% of sulfur could be fixed in the matte and slag phases. In addition, this innovative lead recycling process could simultaneously co-treat jarosite residue and recover some precious metals.

Acknowledgements

The authors thank the Applied Science and Technology Specialized Research Project of Guangdong Province (No.2016B020242001), the National Natural Science Foundation of China (Grant No. 51234009) and CMEco (Grant No. 2116781) for funding this research.

References

[1] X. Tian, Y. Wu, Y. Gong (2015) The lead-acid battery industry in China: outlook for production and recycling, Waste Manage. & Res., 33(11): 986-994.
[2] V.D.K. Tj, L. Huang, C.R. Cherry (2013) Health hazards of China's lead-acid battery industry: a review of its market drivers, production processes, and health impacts, Environ. Health, 12(1): 61.
[3] R. Peng, H.-j. REN, X.-p. ZHANG (2003) Metallurgy of lead and zinc, Science Pres, Beijing, p 250-312.
[4] Q. Zhang (2013) The current status on the recycling of lead-acid batteries in China, Int J Electrochem Sci, 8: 6457-6466.
[5] V. Hotea (2013) Clean Technology of Lead Recovery from Spent Lead Paste, Recent Researches in Applied Economics and Management, Econ. Asp. of Environ., 2: 263-270.
[6] K.-P. Jeong, J.G. Kim (2017) Lead acid battery recycling and material flow analysis of lead in Korea, J. Mater. Cycles and Waste Manage., 1-7.
[7] T.W. Ellis, A.H. Mirza (2010) The refining of secondary lead for use in advanced lead-acid batteries, J. Power Sources, 195(14): 4525-4529.
[8] C. Huang, C. Tang, M. Tang (2012) Sulfur-fixing Reduction Smelting of Spent Lead-acid Battery Colloid Sludge in Fused Salt at Low Temperature, Min. Metall. Eng., 32(2): 84-87.
[9] M.A. Kreusch, M.J.J.S. Ponte, H.A. Ponte (2007) Technological improvements in automotive battery recycling, Resour. Conserv. & Recy., 52(2): 368-380.
[10] A. Singh (2015) Review on Desulfation of Lead-acid Battery for HEV, International Journal of Curr. Eng. and Sci. Res., 2: 85-96.
[11] X. Ma, S. Wang, X. Li (2008) Recycling of lead from the wasted lead-acid battery by solid phase electrolysis, Mater. Res. and App., 2: 141-144.
[12] A. Schröder-Wolthoorn, S. Kuitert, H. Dijkman (2008) Application of sulfate reduction for the biological conversion of anglesite ($PbSO_4$) to galena (PbS), Hydrometallurgy, 94(1-4): 105-109.
[13] D. Lin, K. Qiu (2011), Recycling of waste lead storage battery by vacuum methods, Waste manage., 31(7): 1547-1552.
[14] Y. Hu, C. Tang, M. Tang (2015) Extraction of lead from secondary lead through a low-temperature alkaline and sulfur-fixing smelting process, Chin. J. Eng., 37: 588-594.
[15] Y. Hu, C. Tang, M. Tang (2014) Reductive smelting of spent lead-acid battery colloid sludge in molten salt of sodium at low temperature, China Nonferr. Metal., 43: 75-79.
[16] A. Roine (2002) HSC Chemistry 9.0, Outokumpu Research Oy, Pori, Finland,.
[17] Y. Li, C. Tang, Y. Chen (2017), One-Step Extraction of Lead from Spent Lead-Acid Battery Paste via Reductive Sulfur-Fixing Smelting: Thermodynamic Analysis, Paper presented at the 146th TMS Anuual Meeting, San Diago, California, 26th February-2nd March, 2017.
[18] Li, Y., Chen, Y., Xue, H. (2016) One-step extraction of antimony in low temperature from stibnite concentrate using iron oxide as sulfur-fixing agent. Metals, 6(7): 153-164.